https://doi.org/10.33271/nvngu/2024-1/105

A. Sekhri[*1],
orcid.org/0009-0000-5367-9123,
L. Mahtout[1],
orcid.org/0009-0005-2664-954X,
A. Bouzidi[2],
orcid.org/0000-0002-4616-6896,
N. Bouzidi[1],
orcid.org/0000-0002-9154-5895,
M. Ferfar[3],
orcid.org/0000-0002-2028-5213

1 – Laboratory of Materials Technology and Process Engineering (LTMGP), University of Bejaia, Bejaia, Algeria
2 –Electrical Engineering Laboratory (LGE), University of Bejaia, Bejaia, Algeria
3 – Environmental Research Center, Annaba, Algeria
* Corresponding author e-mail: abderraouf.sekhri@univ-bejaia.dz

ENHANCEMENT OF SORPTION OF THE AZOIC DYE (AZUCRYL RED) BY NATURAL AND CALCINED HYPER-ALUMINOUS KAOLINS

Purpose. To remove of basic textile dye Azucryl Red (AR) from aqueous solutions using hyper-aluminous kaolins from Charente deposits (France) in natural and calcined states.

Methodology. Batch interactive parameter pH, pH_{pzc} contact time, dye concentration, adsorbent loading and temperature are taken to obtain optimums for the AR adsorption process in natural and calcined kaolin named respectively Kca, Kcm, Ckca, and Ckcm.

Findings. The adsorption equilibrium was established in 7 min while the second-order kinetic model better described the adsorption kinetics for all kaolins with the chemisorption process. The adsorption isotherm of the results obtained corresponds better to the Langmuir model. The maximum quantity retained was 67.97 and 73.38 mg/g respectively for Kcm and Kca samples. Moreover, in the calcined state, the maximum quantity retained was 76.66 and 75.64 mg/g respectively for the calcined kaolin CKcm and CKca samples for a temperature of 298 K and pH = 6. The thermodynamic nature of the adsorption process was determined by calculating ΔH, ΔS and ΔG° values. The positive value of ΔH° confirms the fact that adsorption is endothermic spontaneous which is enhanced at higher temperatures.

Originality. The heat treatments of the different kaolins at 400 °C enhance the adsorption process. Therefore, the results indicate that $q_e^{Ckcm} / q_e^{kcm} > q_e^{Ckca} / q_e^{kca}$. Ckcm performed with the highest adsorption capacity in the removal of the dye, followed by Ckca.

Practical value. Adsorption processes of toxic Azucryl Red dye in the aqueous medium using natural and calcined hyper-aluminous kaolins at 400 °C were investigated. Optimization and modeling of the adsorption parameters with the theories by Langmuir, Freundlich and Elovich allowed us to find the optimal experimental conditions for sorption. Our results therefore indicate that the adsorption process of Azucryl red dye from aqueous solutions was enhanced when calcined kaolin at 400 °C containing organic matters was used.

Keywords: *kaolins, Charente basin, calcination adsorbents, Azucryl red dye, adsorption, environment*

Introduction. Large amounts of dye wastewater have been produced as a result of the overuse of synthetic dyes in numerous sectors. A lot of them are made to be harmful and must be disposed of carefully before being disposed of in the receiving bins. Different kinds of dyes are employed in sectors including the processing of chemicals, and the textile industry.

Lotfi, M., et al. [1] claims that to dye 1 kg of cotton with reactive colors, 70 to 150 L of water, 0.6 kg of sodium chloride, and 40 g of reactive dye are normally required. Due to the contribution of toxicity, high organic load, and color-related aesthetic pollution, the effluents containing dyes are very colored and seriously harm the ecosystem and human health during the dyeing and finishing phases, especially with colored products where up to 20 to 30 percent of these applied dyes (approximately 2 g/L) are not fixed to the fabric [2]. The majority of synthetic dyes contain aromatic azo groups, which are extremely harmful to the environment because of their mutagenic, carcinogenic, and inert characteristics [3].

Dye physicochemical, optical, and thermal stability as well as resistance to traditional wastewater treatment are all products of the complex aromatic structures [4]. Compared to anionic dyes, cationic dyes are more poisonous [5]. One of the more well-known cationic dyes is Azucryl Red (AR); its structure is depicted in Fig. 1. It is extensively used in paper printing and textile dyeing.

Treatment of effluents using the adsorption method has proven to be quite effective by using mass transfer to remove dissolved components [6]. Whereas water recovery is crucial, sorption is used in the textile, leather, dyeing, cosmetics, plastics, food, and paper industries [7].

The sorption of organic molecules to an adsorbent depends on various physical and chemical factors [8]. The fixing of chromophore groups of dyes such as azo, anthraquinone, triarylmethane, phthalocyanine, formazan, and oxazine, leads to a covalent bond with the fiber, which gives them a good solubility in water, disappearing in the dye. Those dyes resist washing and exhibit good affinity [9]. The general formula of these dyes is represented as $ArN^{+}RX^{-}$, with R^{-} radical alkyl, X = Cl or, Ar: phenyl radical [10].

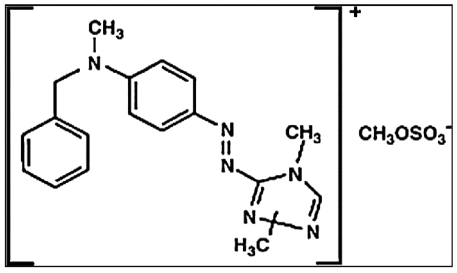

Fig. 1. Chemical structure of AR

Due to their large specific surface area, a variety of natural adsorbents as Bentonite, montmorillonite, alunite, sepiolite, zeolite, kaolinite, and diatomite have been studied to its uses for the removal of dyes from wastewater. However, a dye with an opposite ionic character will adsorb over a highly ionic surface most effectively and quickly [11].

Kaolinite is a 1:1 aluminosilicate with an equidistance of approximately 7Å and is dioctahedral type (one in three octahedral sites remains vacant) [1]. The three sites of the layer octahedral are therefore filled with two aluminum cations and the third site is incomplete. The position of vacant sites, allows differentiating type 1 : 1 mineral kaolinite dickiteand nacrite. The basal surfaces are of two types, consisting of either oxygen ions organized in a hexagonal network, or OH in a compact assembly [12].

A number of sorption-related factors, including contact time, amount of adsorbent, initial pollutant concentration, pH, and temperature were investigated. Three distinct kinetic models for the dye's adsorption are displayed. With the use of the Langmuir, Freundlich, and Elovich isotherm models, the equilibrium data are tested. This foundational research will be useful in developing a batch adsorbed for the treatment of effluent containing dyes coming from dyeing industry.

The aim of this work was to investigate the potential adsorption of cationic dye on hyper-aluminous kaolin naturally rich in gibbsite and organic matters named Kca, Kcm respectively. Calcination of the two kaolin at 400 °C named Ckca and Ckcm were also used in this study for the adsorption process of the cationic dye. Calcination of the clays is part of the current trends seeking to improve their surface area. These materials go through physico-chemical changes that affect both the microstructure and the crystal structure of the various phases (dehydroxylation, amorphization, crystallization, allotropic transformation, decarbonization) [12]. Calcinations of the two kaolins lead to the release of organic matter materials and gibbsite.

Materials and methods. Two French kaolins from Charente basin were used in this study, namely Kca and Kcm. They are composed mainly by kaolinite associated with impurities such as organic matter (Kcm), and gibbsite (Kca). The kaolins were manually milled in a porcelain mortar, then sieved to 63 μm sieve, and dried at 105 °C for 24 h. Analytical grade Azucryl Red ($C_{18}H_{21}BrN_6$) is provided by ALFADITEX (Algerian Textile company). The kaolins were subjected to calcinations in a Nabertherm electric kiln furnace at 400 °C during 2 hours, with a heating rate of 10 °C/min.

1. Mineralogical analysis of the raw materials were carried out by X-ray diffraction (XRD) PANalytical powder diffractometer, monochromatic Cu-Kα1 radiation, of wavelength λ = 1.54 Å and a counting time of 10 s per step. The diffractograms were recorded from 5 to 80° (2θ) with a step of 0.01°.

2. Chemical composition of the kaolins was conducted by X-ray fluorescence (XRF) PANalyticalPerl'X 3 XRF spectrometer.

3. The raw materials (calcined and uncalcined) were prepared and shaken for 24 h at 30 °C (Labwit ZWY-304); after 24 h, the dispersion was filtered through a Millipore 0.45 μm (Z227366 – Millex syringe filter units); and the pH of the filtrate was determined with a Jenway 3010 digital pHmeter.

4. The dosage of dye solution is carried out using a UV – visible spectrophotometer (PerkinElmer Precisel, Lamda-35) at a wavelength of 543 nm.

5. The textural characterization is carried out by the adsorption isotherms; the specific surface was obtained according to the Brunauer-Emmett Teller (BET) method using Quantachrome NOVA Win 2 Analyzer. The total pore volume, average pore radius and micropores were obtained from the adsorption isotherms of the materials. Mesopore volume is determined by subtracting the micropore volume from the total pore volume.

Experimental protocol. A quantity of 0.5 g of natural and calcined Kaolin are introduced in Erlenmeyer flasks with 50 mL of (AR) solution at concentrations 20, 40, 60 and 80 ($mg \cdot L^{-1}$). To estimate the pH and PH_{PZC} of Kca, Kcm, CKca and CKcm dispersion, the following procedure was adopted. The pH of the solution was adjusted with 0.1 M for both NaOH and HCl. The heterogeneous mixture was shaken at 300 rpm in a rotary shaker at 20 ± 1 °C for 24 h to confirm that sorption equilibrium was reached. A volume of 8 ml of the solution (solid/liquid) was taken and centrifuged with centrifuge at 5,000 rpm for 4 minutes. The floatables particles were then filtered using a millipore filter of 0.45 um. The residual adsorbate concentrations are obtained by UV-Visible spectro-photometry for (AR) after establishing a calibration curve. All manipulations were executed in triplicate, the median values were noted to represent a result, and all data was calculated. The quantity (q_t) of (AR) retained at the time (t) on the absorbent is given by the following equation

$$q_t = \frac{C_i - C_t}{m} \cdot V, \qquad (1)$$

where m is the mass of the clays (g); C_i is the starting amount of the colorant; C_t is the amount of dye present at time t ($mg \cdot L^{-1}$); V is the total volume of the solution (L).

The efficiency of the adsorption reaction (% elim) is expressed by the ratio of the amount of (AR) adsorbed to the initial amount of (AR) in the aqueous solution.

$$\%elim. = \frac{C_i - C_e}{C_i} \cdot 100, \qquad (2)$$

where C_e ($mg \cdot L^{-1}$) denotes the concentration of the (AR) in the solution at a state of equilibrium and C_i ($mg \cdot L^{-1}$) indicates the initial concentration of the (AR) in the solution.

Technical methods. ***Dye concentration and removal capacity.*** Stock solutions of Azucryl Red ($C_{18}H_{21}BrN_6$) were prepared by adding 1,000 mg of dye powder 1L of distilled water. The stock dye solutions were precisely diluted to a range of initial concentrations to obtain the son dye solutions. A maximum absorbance of 534 nm was used to quantify the dye concentration colorimetrically.

By diluting a stock solution with a concentration of 100 mg/L at pH 2, 4, 6, 8 and 10, standard solutions with concentrations (AR) ranging from 0.1 to 5 mg/L were obtained. These solutions were then evaluated at the wavelength (max 534 nm) corresponding to the maximum absorption of Azucryl red. Absorbance and concentration of the sample were plotted on a calibration curve of the dye solution to obtain an absorbance–adsorbate profile at different pH.

Error analysis. Over the years, linear regression of the isotherm model was commonly used to select the most suited model; and the method of least squares has often been used to discover the parameters of the models. Chi-square (x^2) test was employed as a criterion for the quality of fitting. This factual investigation is based on the entirety of squares of contrasts between test information and information inferred from calculations, with each squared contrast being partitioned by the comparing information inferred from calculations [13]. The equation can be utilized to represent the Chi-square

$$x^2 = \sum\left(\frac{(q_e - q_t)^2}{q_t}\right), \qquad (3)$$

where q_t was the equilibrium capacity (mg/g) derived from the experimental data and q_e was the equilibrium capacity (mg/g) determined from the model whether experimental data and model data were comparable. A small number shows that the model's data and the experimental value are comparable, but a big value of x^2 highlights the discrepancy between the two. The data set must be analyzed using the Chi-square test together with the values of the determined coefficient (R^2) in order to verify the best-fit isotherms and kinetic models for the adsorption system.

Results and discussion. Chemical composition of the Kca and Kcm samples used for sorption experiments is shown in Table 1. The analysis has reported that the major phases of samples composed mainly silica and alumina, which accounted for 82.53 and 76.08 % of Kca and Kcm respectively of the total mass; such values are similar to those given by Lotfi Mouni, et al., 2018 [1]. The content of Fe_2O_3 is higher in Kcm (1.13 %) than in Kca (0.46 %), this gives a reddish to a dark color to Kcm sample; whereas, the color of Kca is white. Loss on ignitions (L.O.I) of the two kaolin is higher than in ordinary kaolin (~12 %); they are (20.74 %) for Kcm and (16 %) in Kca.

The X-ray diffraction patterns of kaolins showed that Kca and Kcm contain the largest amount of kaolinite (85 and 80 %) respectively, the minor phases observed in Fig. 2, *A* are rutile (2 %), gibbsite (12, 4 %) and organic matters (0.4, 13.6 %) in Kca and Kcm samples respectively. We noticed the decomposition of the gibbsite after the calcination at 400 °C for the two kaolins Kca and Kcm.

The specific surface area of the kaolins was measured using the (BET) method and is 42.003, 13.988 $m^2 \cdot g^{-1}$ for Kca and Kcm respectively shown in Figs. 2, C_1 and C_2. The corresponding pore volume was approximately ~0.276 for Kca and ~0.226 $cm^3 \cdot g^{-1}$ for Kcm in the saturation ($p/p_0 = 0.985$). The average pore diameter calculated according to the (BJH) method is ~10.4, 11.1 nm for Kca and Kcm respectively indicating the mesoporous character of the clays. Indeed, the cumulative pore area determined by the BJH method is (47.002, 16.867 $m^2 \cdot g^{-1}$) respectively for (Kca, Kcm), it was greater than that determined by the BET method, indicating that the clays containing both mesopores and micropores [14].

Fig. 2, *B* shows DTA curves that illustrate many changes that occur during the calcination of Kca and Kcm. The dehydration of gibbsite ($Al(OH)_3$) to produce a transition alumina phase is responsible for the endothermic peak seen in the Kca sample at about 295 °C. In contrast, the Kcm sample exhibits an exothermic peak around 350 °C, which is due to the breakdown of organic maters.

Effect of contact time on AR removal. Fig. 3, *a* shows how contact time affects the systems (AR) solution/Kca, Kcm, CKca and Ckcm. The testing was done in a batch manner. It indicates that adsorption occurred after only a short time of equilibrium, indicating that all adsorbents reduced (AR) from water very instantly. After the 7 minutes, sorption slows down

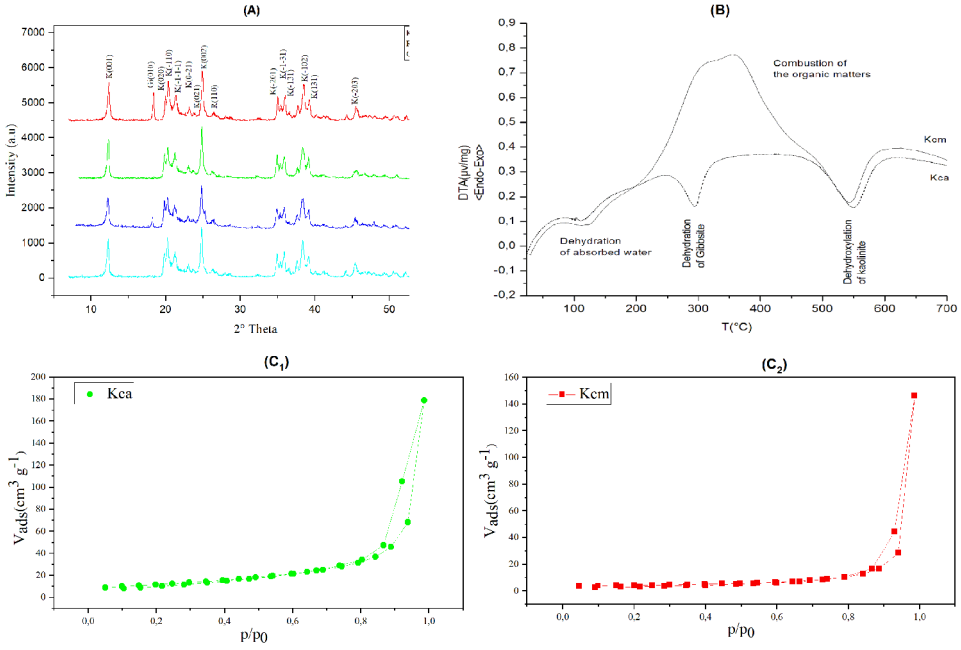

Fig. 2. Characterization of the natural and calcined kaolin:

a – X-ray diffractogram; b – DTA curves; c – Nitrogen adsorption and desorption isotherms

Table 1

Chemical and mineralogical compositions of the kaolin

Chemical compositions of the kaolin											
Oxides (%)	SiO_2	Al_2O_3	Fe_2O_3	MnO	MgO	CaO	Na_2O	K_2O	TiO_2	P_2O_5	L.O.I
Kca	40.09	42.44	0.46	0.01	0.05	0.18	0.06	0.04	0.63	0.05	16.00
Kcm	43.17	32.91	1.13	0.13	0.01	0.47	0.06	0.50	0.80	0.10	20.74

Mineralogical compositions of the kaolin				
Mineralogical phases (%)	Kaolinite	Rutile	Gibbsite	Organic matters
Kca	85	2	12	0.4
Kcm	80	2	4	13.6

until equilibrium is achieved with adsorption capacities of 76.7 for Ckcm, 75.6 for Ckca, 73.4 for Kca and 67.9 mg · g^{-1} for kcm, respectively. Such values are significantly higher than those that are reported by Hongxia, et al. [15]. Compared to Kca, Kcm provides better performance adsorption efficiency after heat treatment; we have also observed a little increase in the capacity. Heat treatment is recognized as a means of improving the adsorption characteristics of raw kaolin.This explains the increase in the exchange force difference between the concentration of the solution and the surface/interface of the kaolin calcined and uncalcined in the first 7 min. The adsorption speed becomes slow after equilibrium time due to the increased competition of the active adsorption process.

Effect of pH and pH_{PZC} on AR adsorption. The adsorption behaviors of (AR) on the kaolin calcined and uncalcined were studied over a wide pH range of 2–10 Fig. 4, *a*. The highest sorption capacity was noted at pH = 10 for all simple Kaolin. The most adsorption efficiency amounted to 99.09 mg · g^{-1} for Ckca; such values are similar to those given by Lotfi Mouni [1]. Comparing with Ckcm, Kca and Kcm, we noticed a slight decrease in the adsorption capacity (98.9, 97.5 and 91.02 %) respectively. For kaolin Kca and Kcm, the point of zero charge is estimated to be as 5.7 and 6 respectively (Figs. 4, *c* and *d*). However, we noted pH_{PZC} 5.4 and 6.4 for the samples Ckca and Ckcm respectively. Generally, at pH > pH_{PZC} the Kaolin samples can acquire negative surface charges leading to a stronger electrostatic attraction and positive auxochromic groups of cationic dye (AR). Therefore, pH ~ 10 was obtained to be the best solution pH for the removal of Azucryl red dye. At pH < pH_{PZC}, the dye molecules carried a positive charge and also the surface of the adsorbent [16].

Influence of adsorbent loading. Effect of the ratio dose (*Radsorbent/solution*) varying from 0.5 to 2.0 g · L^{-1} on the dye uptake is shown in Fig. 3, *b*. According to the results obtained, the dye uptake (80 mg · g^{-1}) decreases with an increase in kaolin calcined and uncalcined dose, the maximum capacity of removal dye was observed at *R* ratio 0.5g/L for Ckcm 400 (73.29 mg · g^{-1}), also Ckca 400 capacity (72.31 mg·g^{-1}) approach to Ckcm 400 to uptake dye, so the heat treatment brought an upgrade in the efficiency of sorption capacity; comparing with raw kaolin Kca and Kcm we noticed low capacity (67.83, 64.86 mg · g^{-1}) respectively. Further, an increase in adsorbent dosage above 0.5 g did not show any further improvement in (AR) dye removal. Therefore, 0.5 g was chosen to be an optimum adsorbent dosage for further investigations. This behavior can be explained by the agglomerations of crystals when the ratio of adsorbent/solution increases [16].

Effect of initial basic dye concentration. From the results shown in Fig. 3, *d* of experiments dye concentration varies from 20 to 80 mg · L^{-1}. Dye removal tended to increase when the initial dye concentration increased until reaching an elimination rate (76.64 and 75.62 mg · g^{-1}) for Ckcm and Ckca respectively at 80 mg · g^{-1} of dye concentration. The greatest adsorption was shown by the raw kaolin Kca and Kcm 67.83 and 64.86 mg · g^{-1} respectively. This may be attributed to the greater concentration gradient that acts as an actuation to move the (AR) dye molecules toward active adsorption sites in heat-treated kaolin. Feriel, et al. [11] founds results similar to these values at 400 °C of calcination.

Effect of temperature. Batch adsorption tests in the temperature range of 293–345 K were carried out to study the impact of temperature on the sorption abilities of raw kaolins and calcined kaolins for (AR). The results are given in Fig. 3, *c*. All simple kaolins have been found to have an increased adsorption capability with rising temperatures. The fact that the viscosity of the solution reduces with rising temperature made this behavior obvious. This is advantageous for the succeeding sorption stages of transfer to the outside and dispersion of the adsorbate within the adsorbent solid. This rise is probably due to: a) the increase in the mobility of the dye, allowing it to cross the pores of the sample; b) the rise in the chemical relationship between the adsorbate and the surface functionalities of the adsorbent; c) the variation of chemical potentials, correlated to the solubility of the adsorbed species.

Adsorption isotherm. Three well-known models, the Freundlich, Langmuir [17], and Elovich isotherms, were used to illustrate dye-clay interaction in this research in order to evaluate the interaction between adsorbate molecules and adsorbent surface.

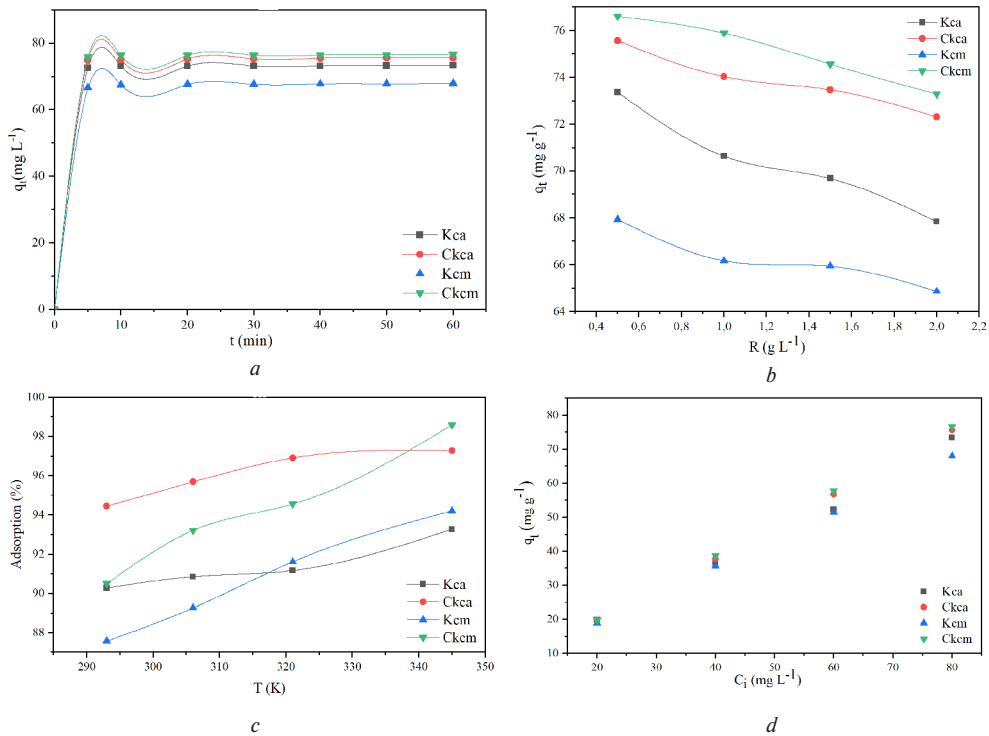

Fig. 3. Effects:

a – effect of contact time; b – effect of ratio R ($m_{adsorbent}/V_{solution}$) on the adsorption capacity; c – influence of temperature on AR dye removal efficiency; d – effect of the mass of adsorbent on the amount of AR adsorbed

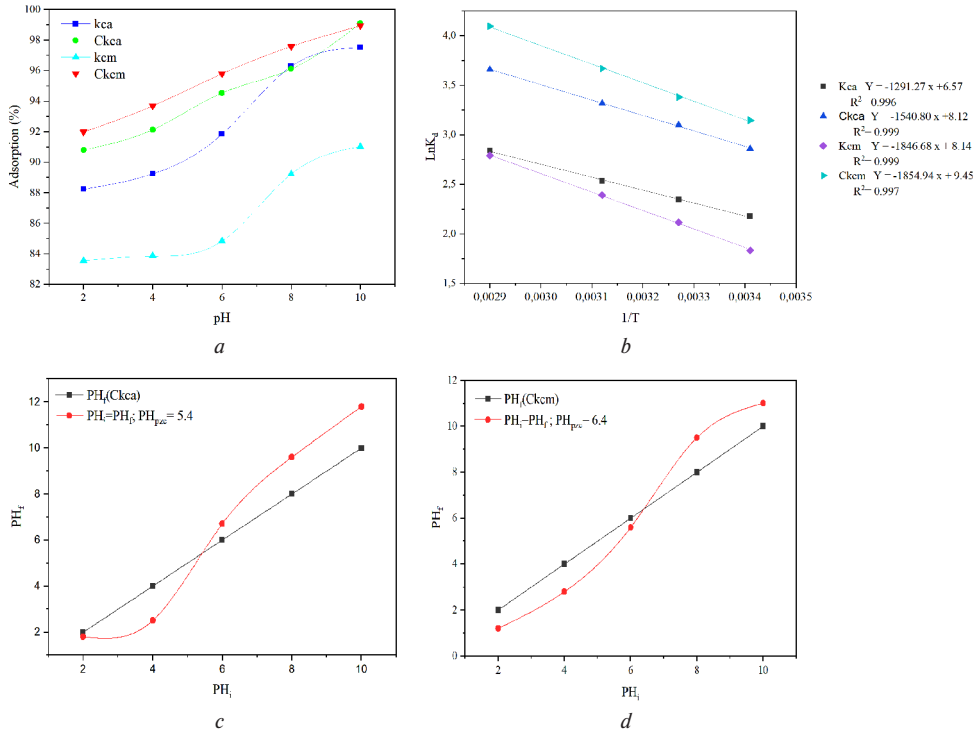

Fig. 4. Effects:

a – effect of pH on AR adsorption; b – projection of lnKdvs reciprocal temperature (1/T); c – point of zero charge (pH_{ZPC}) *of Kca; d – point of zero charge* (pH_{ZPC}) *of Kcm*

Freundlich isotherm. The model can be expressed as

$$q_e = K_F C_e^{1/n}. \tag{4}$$

It can be linearized by

$$\log q_e = \log K_F + \frac{1}{n}\log C_e, \tag{5}$$

where C_e is the concentration of dye solution at adsorption equilibrium (mg · L^{-1}); q_e is the quantity of dye adsorbed per unit of adsorbent; KF ($mg^{1-1/n}l^{1/n}g^{-1}$) and n are the constants of Freundlich. This model can be described as a physical process and is favorable if n is greater than unity.

Langmuir isotherm. The Langmuir isotherm is based on the notion that the monolayer coverage and the adsorbent are structurally homogenous. The model can be expressed as

$$\frac{c_e}{q_e} = \frac{1}{q_{\max}} c_e + \frac{1}{K_L q_{\max}}. \tag{6}$$

The linearized equation is

$$\frac{1}{q_e} = \frac{1}{q_m} + \frac{1}{K_L q_m} - \frac{1}{C_e}, \tag{7}$$

where K_L is the constant of Langmuir ($l\ mg^{-1}$); q_m is the maximum quantity of adsorption necessary to completely cover a monolayer on the adsorbent surface (mg · g^{-1}). The linear plot of $1/C_e$ vs $1/q_e$ can be applied to calculate the Langmuir constants KL and q_m. According to [17], the equitable adsorption of the Langmuir isotherm may be defined in terms of the equilibrium parameter R_L, which is a dimensionless constant separation factor.

$$R_L = \frac{1}{1 + K_L C_i}, \tag{8}$$

where C_i (mg · l^{-1}) is the initial (AR) concentration. The parameter values may be roughly divided into four categories, which represent the isotherm's shape: $R_L > 1$ indicates an unfavorable isotherm; $R_L = 1$ indicates a linear isotherm; $0 < R_L < 1$ indicates a favorable isotherm, and $R_L = 0$ indicates an irreversible isotherm.

Elovich isotherm. The Elovich isotherm is expressed by the following relation

$$\frac{q_e}{q_m} = K_E C_e e^{\frac{-q_e}{q_m}}. \tag{9}$$

The equation can be linearized as

$$\ln\left(\frac{q_e}{c_e}\right) = \ln(K_e q_m) - \left(\frac{q_e}{q_m}\right), \tag{10}$$

where q_m (mg · g^{-1}) is the maximum quantity adsorbed per unit mass of the adsorbent; K_e (L · mg^{-1}) is the constant of Elovich.

As illustrated in Fig. 5, the linear regression of Langmuir Fig. 5, *a*, Freundlich Fig. 5, *b* and Elovich Fig. 5, *c* for the adsorption of (AR) onto natural (Kcm, Kca) and calcined kaolin (CKcm, CKca), is well fitted to the linear Langmuir isotherm. When the Langmuir model (Table 2) was used to describe the adsorption of Azucryl red onto natural kaolin and calcined kaolin. The high value of $R_2 > 0.990$ and smaller values of χ^2 were observed for all kaolins in the Langmuir model. The maximum adsorption capacity q_m was 94.76 and 86.28 mg · g^{-1} onto calcined Kaolins Ckcm, Ckca respectively for the Langmuir model indicating the homogeneous active sites and monolayer coverage of AR onto the kaolins surface. The Freundlich coefficient value 1/n (indicative of favourability when $0.1 < 1/n < 1$) is more favorable in Ckcm and Ckca (Table 2) compared with natural kaolins. Therefore, the Freundlich model is still a good model to describe the adsorption data. However, the R^2 and χ^2 values of Elovich are close to the R^2 and χ^2 values in the Freundlich model, which shows poor linearization compared to the Langmuir isotherm for natural and calcined clay.

Thermodynamic analyses. Thermodynamic parameters were determined as follow

$$\Delta G^\circ = \Delta H^\circ - \Delta H^\circ \cdot T. \tag{11}$$

And the van't Hoff equation as

$$\ln K_d = \frac{\Delta S^\circ}{R} - \frac{\Delta H^\circ}{R.T}, \tag{12}$$

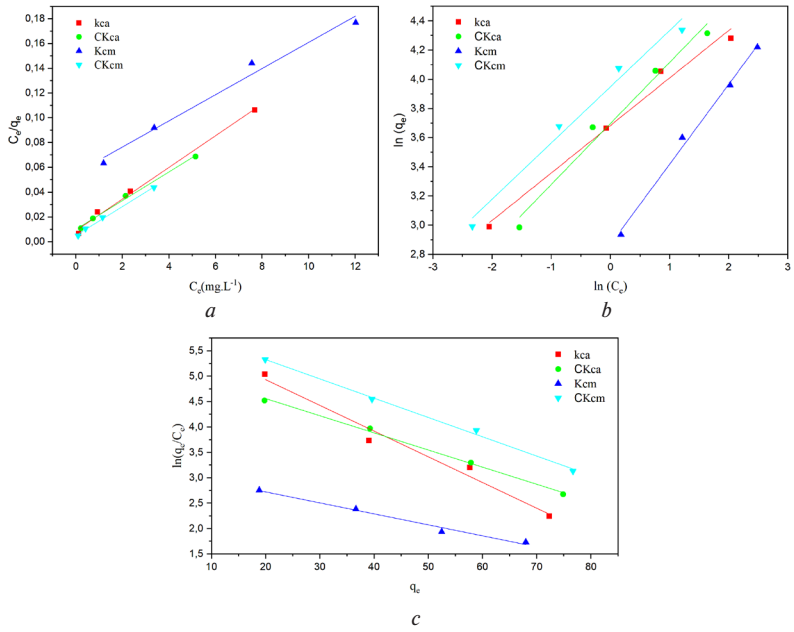

Fig. 5. Langmuir (a), Freundlich (b) and Elovich (c) isotherms for the adsorption of AR onto natural and calcined kaolin

Table 2

Constants for both models of adsorption: Langmuir, Freundlich and Elovich for natural and calcined kaolin

Material	Langmuir				Freundlich					Elovich		
	K_L	q_m	R^2	χ^2	K_F	$1/n$	R^2	χ^2	q_m	K_e	R^2	χ^2
Kca	1.438	78.248	0.992	0.220	39.815	0.418	0.978	0.407	9.755	0.301	0.964	0.482
CKca	1.160	86.281	0.994	0.221	40.372	0.326	0.969	0.587	29.656	0.176	0.974	0.423
Kcm	2.309	85.697	0.994	0.205	17.620	0.584	0.970	0.426	46.274	0.07	0.976	0.406
CKcm	0.191	94.763	0.994	0.222	51.901	0.385	0.973	0.401	26.329	0.231	0.963	0.534

where K_d is the equilibrium constant, which is the difference between the equilibrium concentration of basic dye in solution and the equilibrium concentration of those ions attached to the adsorbent; T is the adsorption temperature in Kelvin; R is the constant gas ideal. The values of ΔH° (kJ · mol^{-1}) and ΔS° (J mol^{-1} · K^{-1}) are determined from the slope and intercept of the van't Hoff plots, and the plot of $\ln K_d$ vs $1/T$ should result in a straight line (Fig. 4, *b*). The endothermic adsorption process is shown by the positive values of ΔH° in Table 3. The negative values of ΔG° showed that for the natural and calcined kaolin samples adsorbent was successful, indicating spontaneous adsorption in removing AR dye from the aqueous phase, and, as anticipated, performed favorably in comparison to other clay materials [1].

Adsorption kinetics. Different kinetic models are used to investigate the mechanisms of the Azucryl red adsorption process on the surface of kaolin.

Pseudo-first-order kinetic model. The differential equation that corresponds to this model is defined as

$$\ln(q_e - q_t) = \ln(q_e) - K_1 t, \qquad (13)$$

where q_e and q_t are the quantities of Azucryl red adsorbed (mg · g^{-1}) at equilibrium; at time t (min), respectively; K_1 is the adsorption rate constant (min^{-1}). The values of K_1 and q_e were calculated from the slope and the intercept of the plots of $\ln(q_e - q_t)$ as a function of (t) respectively at different kaolin, Fig. 6. As shown in Table 4, the first-order kinetic curves of all kaolin did not fit well the data with a low R^2 value ($R^2 < 0.97$) and the calculated value of q_e^{cal} does not agree with the $q_e^{\exp}$. It may be concluded that the kinetics of Azucryl red adsorption on all kaolins (natural and calcined) does not follow the pseudo-first-order kinetic model [16].

Pseudo-second-order kinetic model. The sorption kinetics of the pseudo-second-order model is as follows

$$\frac{t}{q_t} = \frac{t}{q_e} + \frac{1}{K_2 (q_e)^2}, \qquad (14)$$

where K_2 (min^{-1} · g · mg^{-1}) is the adsorption rate constant of the pseudo-second-order adsorption rate. The value of q_e and K_2 can be obtained from the slope and the intercept of the plot of (t/q_t) versus t respectively where K_2 (min^{-1} · g · mg^{-1}) is the adsorption rate constant of the pseudo-second-order adsorption rate. Table 5 displays the computed values for k_2, q_e, and the related regression coefficient (R^2) values. The regression coefficient's value of the sorption for Azucryl red by Kca, Ckca

Table 3

Thermodynamic parameters for adsorption of AR on natural and calcined kaolin

Material	ΔG° (J · mol^{-1})				ΔH° (kJ · mol^{-1})	ΔS° (J mol^{-1} · K^{-1})	R^2
	293 (k)	306 (k)	321 (k)	345 (k)			
Kca	–5,305.51	–5,969.02	–6,762.22	–8,151.18	10.74	54.65	0.996
Kca 400	–6,966.97	–7,884.32	–8,856.05	–10,492.53	12.81	67.54	0.999
Kcm	–4,470.25	–5,387.49	–6,380.76	–7,999.32	15.35	67.71	0.997
Kcm 400	–7,662.78	–8,598.71	–9,792.05	–11,743.15	15.42	78.64	0.999

and Kcm, Ckcm is nearly unity (0.99) as shown in Fig. 7. However, demonstrating that the compound's sorption kinetics is consistent with a pseudo-second-order mechanism. Table 5 further shows that the estimated q_e^{cal} values are extremely similar to the q_e^{exp} that was achieved experimentally. Thus, it can be inferred that a pseudo-second-order kinetic model may explain the adsorption of Azucryl red on kaolins more effectively than a first-order kinetic model, and the process is chemisorption managed [18].

The following relationship explains how intra-particle diffusion resistance affects adsorption

$$q_t = K_{di} t^{0.5} + C, \quad (15)$$

where q_t is the amount adsorbed at time t; $t^{0.5}$ is the square root of the time; K_{id} is the rate constant of intra-particle diffusion; C is the intercept that represents the boundary layer thickness.

As shown in Fig. 8, the curves do not pass by the origin; this indicates that intra-particle diffusion is not the only phase that determines the sorption kinetics of (AR). This corroborates the hypothesis that the ions absorb on the adsorption sites present on the surface of the solid (mesopores). According to the intra-particle diffusion rate constants (Table 6), the film diffusion takes place simultaneously with intra-particle diffusion. Thus, both can be considered as the rate-controlling steps of the adsorption for natural and calcined kaolins studied in this work [19].

Conclusion. The efficiency of the basic dye adsorption on calcined kaolins (400 °C) was confirmed. Different parameters such as initial concentration of dye (20 to 80 mg · L^{-1}), pH (2 to 10), ratio R ($m_{adsorbent}/V_{solution}$) (0, 5 to 2 g · L^{-1}) and temperature (20, 33, 48 and 72 °C) were optimized in order to obtain the best operating conditions of Azucryl red (pH = 6, T = = 25 °C, $R_{S/L}$ = 0.5 g/L, C_0 = 80 mg/L and contact time = = 60 min). After the first 7 minutes, sorption slows down until equilibrium is achieved with adsorption capacities of 76.7 for Ckcm, 75.6 for Ckca, 73.4 for Kca, and 67.9 mg · g^{-1} for Kcm. The adsorption isotherm of the results obtained corresponds better to the Freundlich model. The maximum quantity retained was 76.66 and 75.64 mg/g respectively for the calcined kaolins CKcm and CKca, which really illustrates the efficiency of heat treatment at 400 °C in sorption of basic dye (Azucryl Red).

The pseudo-second-order model equation provided a good description of the adsorption kinetics. The Langmuir model successfully adjusted an adsorption isotherm. The process of adsorption for natural and calcined kaolin is managed

Table 4

Parameters of the kinetic pseudo-first-order model for the adsorption of AR on the natural and calcined kaolin

Pseudo-first order model																
C_i (mg L^{-1})	Kca				Ckca				Kcm				Ckcm			
	q_e^{exp}	q_e^{cal}	K_1	R^2	q_e^{exp}	q_e^{cal}	K_1	R^2	q_e^{exp}	q_e^{cal}	K_1	R^2	q_e^{exp}	q_e^{cal}	K_1	R^2
20	19.87	1.06	0.03	0.96	19.80	0.77	0.04	0.81	18.89	0.95	0.03	0.95	19.8	0.93	0.04	0.81
40	36.65	0.83	0.03	0.96	37.74	1.15	0.06	0.83	35.66	1.02	0.03	0.97	38.73	0.78	0.04	0.95
60	52.27	0.54	0.04	0.81	56.72	0.9	0.04	0.96	51.15	0.39	0.04	0.62	57.69	0.7	0.03	0.84
80	73.38	0.56	0.03	0.75	75.64	1	0.05	0.86	67.98	1.06	0.04	0.8	76.66	0.63	0.02	0.72

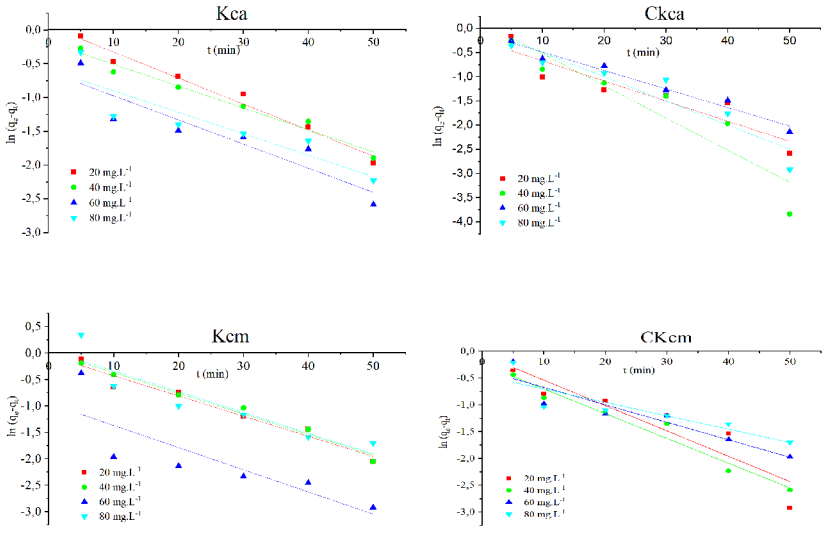

Fig. 6. Plots of the pseudo-first-order model for the adsorption of AR on the Kcm, CKcm, Kca and CKca

Table 5

Parameters of the kinetic pseudo-second-order model for the adsorption of AR on the natural and calcined kaolin

Pseudo-second order model																
	Kca				Ckca				Kcm				Ckcm			
C_i (mg L^{-1})	q_e^{exp}	q_e^{cal}	K_2	R^2	q_e^{exp}	q_e^{cal}	K_2	R^2	q_e^{exp}	q_e^{cal}	K_2	R^2	q_e^{exp}	q_e^{cal}	K_2	R^2
20	19.87	19.93	0.11	0.99	19.80	19.84	0.16	0.99	18.89	18.94	0.12	0.99	19.8	19.86	0.14	0.99
40	36.65	36.68	0.13	0.99	37.74	37.82	0.15	0.99	35.66	35.72	0.12	0.99	38.73	38.86	0.17	0.99
60	52.27	52.30	0.22	0.99	56.72	56.75	0.13	0.99	51.15	51.23	0.32	1	57.69	57.7	0.16	0.99
80	73.38	75.98	0.19	1	75.64	75.7	0.14	0.99	67.98	68.02	0.12	0.99	76.66	76.68	0.17	0.99

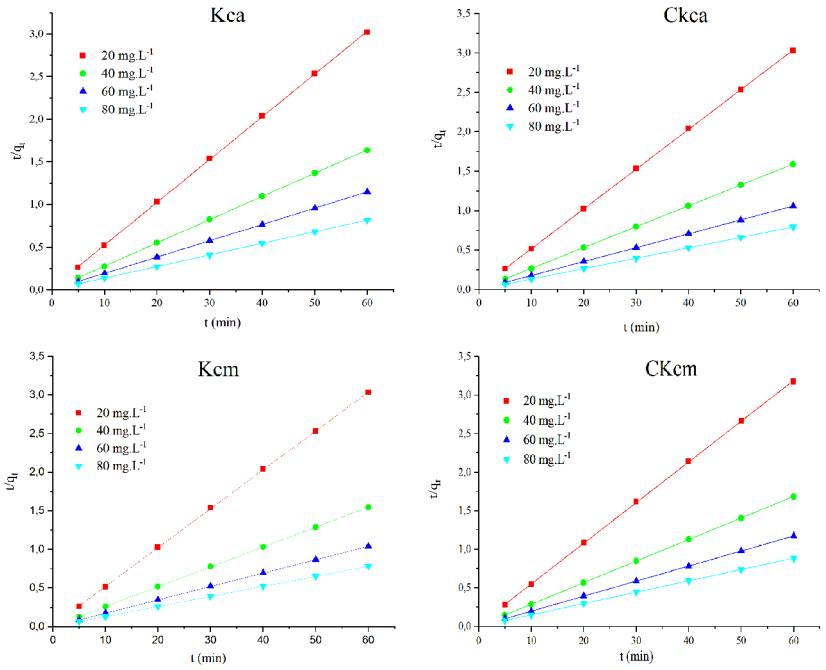

Fig. 7. Plots of the pseudo-second-order model for the adsorption of AR on the Kcm, CKcm, Kca and CKca

Table 6

Intra-particle diffusion rate constants for the adsorption of AR on the natural and calcined kaolin

Intra-particle diffusion model												
	Kca			Ckca			Kcm			Ckcm		
C_i (mg L^{-1})	K_{di}	C	R^2	K_{di}	C	R^2	K_{di}	C	R^2	K_{di}	C	R^2
20	0.15	18.68	0.97	0.12	18.87	0.78	0.14	17.78	0.93	0.12	18.89	0.95
40	0.12	35.66	0.96	0.13	36.8	0.91	0.14	34.53	0.99	0.11	37.98	0.95
60	0.08	51.60	0.78	0.12	55.70	0.97	0.08	50.57	0.51	0.11	56.77	0.79
80	0.09	72.62	0.72	0.12	74.70	0.96	0.19	66.51	0.71	0.10	75.78	0.74

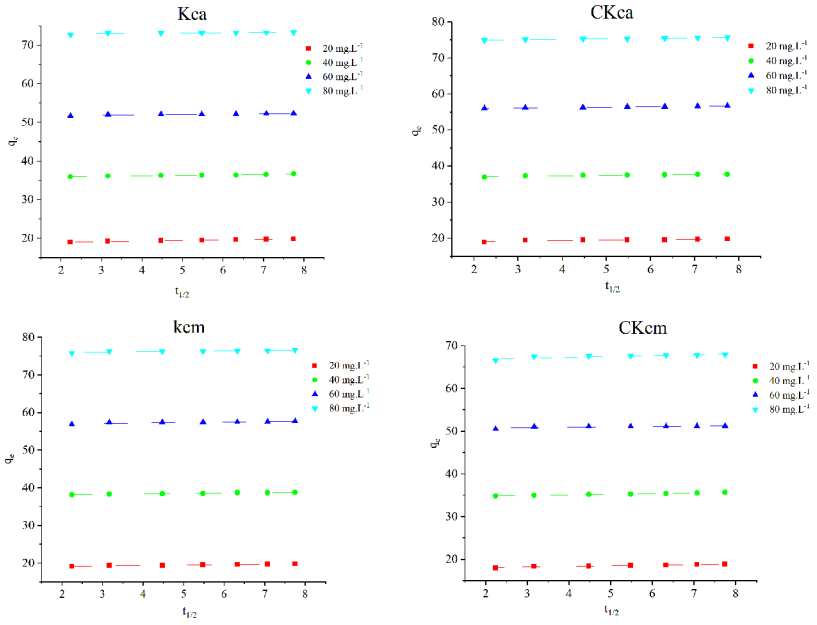

Fig. 8. Plots of the intra-particle diffusion model for the adsorption of AR on the Kcm, CKcm, Kca and CKca

in chemisorption. The values of $\Delta G°$ indicate that the adsorption process is spontaneous. The positive values of both ΔH and $\Delta S°$ show that the adsorption process is endothermic.

The results indicate that $q_e^{Ckcm}/q_e^{kcm} > q_e^{Ckca}/q_e^{kca}$. Ckcm sample presents the highest adsorption capacity in the removal of the dye, followed by Ckca. It can be concluded that the heat

treatment has a positive effect on the enhancement of adsorption performance, due to the combustion of organic matters in Kcm and the release of gibbsite in kca.

References.

1. Lotfi, M., Lazhar, B., Jean-Claude, B., Abdelkrim, B., Aymen, A., Amar, T., Farid, ..., & Houcine, R. (2018). Removal of Methylene Blue from aqueous solutions by adsorption on Kaolin: Kinetic and equilibrium studies. *Applied Clay Science, 153,* 38-45. https://doi.org/10.1016/j.clay.2017.11.034.

2. Errais, E., Duplay, J., & Darragi, F. (2010). Textile dye removal by natural clay – case study of Fouchana Tunisian clay. *Environmental Technology, 31,* 373-380. https://doi.org/10.1080/09593330903480080.

3. Nejib, A., Joelle, D., Fadhila, A., Sophie, G., & Malika, T.-A. (2015). Adsorption of anionic dye on natural and organophilic clays: effect of textile dyeing additives. *Desalination and Water Treatment, 54,* 1754-1769. https://doi.org/10.1080/19443994.2014.895781.

4. Adeyemo, A. A., Adeoye, I. O., & Bello, O. S. (2017). Adsorption of dyes using different types of clay: a review. Applied Water thermodynamic studies. *Chemical Engineering Journal, 155,* 627-636. https://doi.org/10.1007/s13201-015-0322-y.

5. Chaari, I., Fakhfakh, E., Medhioub, M., & Jamoussi, F. (2019). Comparative study on adsorption of cationic and anionic dyes by smectite rich natural clays. *Journal of Molecular Structure, 1179,* 672-677. https://doi.org/10.1016/j.molstruc.2018.11.039.

6. Abida, K., Munawar, I., Anum, J., Kiran, A., Zill-i-Huma, N., Haq Nawaz, B., & Shazia, N. (2018). Dyes adsorption using clay and modified clay: A review. *Journal of Molecular Liquids, 256,* 395-407. https://doi.org/10.1016/j.molliq.2018.02.034.

7. Malakootian, M., Mansoorian, H. J., Hosseini, A., & Khanjani, N. (2015). Evaluating the efficacy of alumina/carbon nanotube hybrid adsorbents in removing Azo Reactive Red 198 and Blue 19 dyes from aqueous solutions. *Process Safety and Environment Protection, 96,* 125-137. https://doi.org/10.1016/j.psep.2015.05.002.

8. Mishra, S., & Maiti, A. (2020). Biological methodologies for treatment of textile wastewater. *Water Science and Technology Library, 91,* 77-107. https://doi.org/10.1007/978-3-030-38152-3_6.

9. Gamoudi, S., & Srasra, E. (2019). Adsorption of organic dyes by HDPy+-modified clay: effect of molecular structure on the adsorption. *Journal of Molecular Structure, 1193,* 522-531. https://doi.org/10.1016/j.molstruc.2019.05.055.

10. Priscila, F. de Sales, Zuy M. Magriotis, Marco Aurélio de L. S. Rossi, Letícia G. Tartuci, ..., & Paulo R. M. Viana (2013). Study of chemical and thermal treatment of kaolinite and its influence on the removal of contaminants from mining effluents. *Journal of Environmental Management, 128,* 480-488. https://doi.org/10.1016/j.jenvman.2013.05.035.

11. Feriel, B., Sonia, D., Neila, D., & Mohamed, F. M. (2015). Application of modified clays as an adsorbent for the removal of Basic Red 46 and Reactive Yellow 181 from aqueous solution. *Desalination and Water Treatment, 29,* 13561-13572. https://doi.org/10.1080/19443994.2015.1061953.

12. Bouzidi, N., Siham, A., Concha-Lozano, N., Gaudon, P., Janin, G., Mahtout, L., & Merabet, D. (2014). Effect of chemico-mineralogical composition on color of natural and calcined kaolins. *Color Research and Application, 39,* 499-505. https://doi.org/10.1002/col.21813.

13. Rumi, G., & Amit, K. D. (2022). Use of Anionic Surfactant-Modified Activated Carbon for Efficient Adsorptive Removal of Crystal Violet Dye. *Adsorption Science & Technology, 28,* 2357242. https://doi.org/10.1155/2022/2357242.

14. Erling, D., Shaoming, Y., Liming, Z., Jinsong, Z., Xiangqi, Huang & Wang, Y. (2011). Pb(II) sorption on molecular sieve analogs of MCM-41 synthesized from kaolinite and montmorillonite. *Applied Clay Science, 51,* 4-101. https://doi.org/10.1016/j.clay.2010.11.009.

15. Hongxia, Z., Zhiwei, N., Zhi, L., Zhaodong, W., Weiping, L., Xiaoyun, W., & Wangsuo, W. (2015). Equilibrium, kinetic and thermodynamic studies of adsorption of Th(IV) from aqueous solution onto kaolin. *Journal of Radio analytical and Nuclear Chemistry, 303,* 87-97. https://doi.org/10.1007/s10967-014-3324-6.

16. Bouatay, F., Dridi-Dhaouadi, S., Drira, N., & Mhenni, M. F. (2016). Application of modified clays as an adsorbent for the removal of Basic Red 46 and Reactive Yellow 181 from aqueous solution. *Desalination and Water Treatment, 57,* 13561-13572. https://doi.org/10.1080 /19443994.2015.1061953.

17. Trevor, C. B., Ali, B., Christopher, M., & Fellows (2023). Universal Langmuir and Fractal Analysis of High-Resolution Adsorption Isotherms of Argon and Nitrogen on Macroporous Silica. *American Chemical Society.* https://doi.org/10.1021/acs.langmuir.2c02932.

18. Elhadj, M., Samira, A., Mohamed, T., Djawad, F., Asma, A., & Djamel, N. (2020). Removal of Basic Red 46 dye from aqueous solution by adsorption and photocatalysis: equilibrium, isotherms, kinetics, and thermodynamic studies. *Separation Science and Technology, 55,* 867-885. https://doi.org/10.1080/01496395.2019.1577896.

19. Feng, N. C., Guo, X. Y., Liang, S., Zhu, Y. S., & Liu, J. P. (2011). Biosorption of Heavy Metals from Aqueous Solutions by Chemically Modified Orange Peel. *Journal of Hazardous Materials, 185,* 49-54. https://doi.org/10.1016/j.jhazmat.2010.08.114.

Посилення адсорбції азоїдного барвника (Azucryl Red) природними та прогартованими гіпералюмінієвими каолінами

А. Сехрі[*1], *Л. Махтут*[1], *А. Бузіді*[2], *Н. Бузіді*[1], *М. Ферфар*[3]

1 – Лабораторія технології матеріалів і технологічного машинобудування (LTMGP), Університет Беджая, м. Беджая, Алжир

2 – Лабораторія електротехніки (LGE), Університет Беджая, м. Беджая, Алжир

3 – Центр екологічних досліджень, м. Аннаба, Алжир

* Автор-кореспондент e-mail: abderraouf.sekhri@univ-bejaia.dz

Мета. Вилучення основного текстильного барвника Azucryl Red (AR) із водних розчинів за допомогою гіпералюмінієвих каолінів родовищ Шаранти (Франція) у природному та прогартованому стані.

Методика. З метою отримання оптимальних значень параметрів процесу адсорбції AR у природному та прогартованому каоліні з відповідними назвами Kca, Kcm, Ckca та Ckcm, використовували інтерактивні параметри pH, час контакту pH_{pzc}, концентрацію барвника, завантаження адсорбенту й температуру.

Результати. Адсорбційна рівновага була встановлена за 7 хв, а кінетична модель другого порядку краще описала кінетику адсорбції всіх каолінів у процесі хемосорбції. Ізотерма адсорбції отриманих результатів краще відповідає моделі Ленгмюра. Максимальна утримувана кількість становила 67,97 і 73,38 мг/г відповідно у зразках Kcm і Kca. Крім того, у прокаленому стані максимальна утримувана кількість становила 76,66 і 75,64 мг/г відповідно для прокалених зразків каоліну CKcm і CKca за температури 298 K і pH = 6. Термодинамічну природу процесу адсорбції визначали шляхом розрахунку значень ΔH, ΔS і ΔG°. Позитивне значення ΔH° свідчить про те, що адсорбція є ендотермічно спонтанною, яка посилюється при підвищенні температури.

Наукова новизна. Термічна обробка різних видів каолінів при 400 °C посилює процес адсорбції. Тому результати показують, що $q_e^{Ckcm}/q_e^{kcm} > q_e^{Ckca}/q_e^{kca}$. Ckcm продемонстрував найвищу адсорбційну здатність у видаленні барвника, за ним слідує Ckca.

Практична значимість. Досліджені процеси адсорбції токсичного барвника Azucryl Red у водному середовищі із застосуванням природного та прогартованого гіпералюмінієвих каолінів при 400 °C. Оптимізація й моделювання параметрів адсорбції за допомогою теорій Ленгмюра, Фрейндліха та Еловича дозволили знайти оптимальні експериментальні умови адсорбції. Таким чином, наші результати свідчать про те, що процес адсорбції барвника Azucryl Red із водних розчинів удосконалюється при використанні прогартованого при 400 °C каоліну, що містить органічні речовини.

Ключові слова: *каоліни, Шарантський басейн, прогартовані сорбенти, барвник Azucryl Red, адсорбція, навколишнє середовище*

The manuscript was submitted 16.08.23.